Compressive Strength of Bottle-Shaped Compression Fields of Fiber Reinforced Concrete Members

Hussein Al-Quraishi
Lecturer
Hussain.abbas@yahoo.com

Ghzwan Ghanim
Assistance Lecture
ghzwannn@yahoo.com

Zinah Asaad
Lecturer
zinaassd46@yahoo.com

Building and Construction Engineering Department, University of Technology/ Baghdad

ABSTRACT

Applying load to a structural member may result in a bottle-shaped compression field especially when the width of the loading is less than the width of bearing concrete members. At the Building and Construction Department – the University of Technology-Iraq, series tests on fibre reinforced concrete specimens were carried out, subjected to compression forces at the top and bottom of the specimens to produce compression field. The effects of steel fibre content, concrete compressive strength, transverse tension reinforcement, the height of test specimen, and the ratio of the width of loading plate to specimen width were studied by testing a total of tenth normal strength concrete blocks with steel fibre and one normal strength concrete block without steel fibres. Based on experimental results; all the test specimens failed with the splitting of concrete directly under the loading plate. Increased the uniaxial compressive strength of concrete increases the maximum bearing capacity of compressive stresses. The load-transverse deformation initially behaves linearly and shows some nonlinearity before failure. Addition of steel fibre to normal strength concrete or presence of transverse reinforcement, delay the reaching of maximum compressive stress after the presence of the first crack.

Keywords: Fiber reinforced concrete, compressive stresses, bottle shaped compression field.

مقاومة الانضغاط للمجال الانضغاطي على شكل قنينة للاعضاء الخرسانية المسلحة بالالياف

حسين القريشي
مدرس

غزوان غانم
مدرس مساعد

زينة اسعد
مدرس

قسم هندسة البناء والإنشاءات، الجامعة التكنولوجية/ بغداد

الخلاصة

عند تسليط الحمل على العضو الانشائي يمكن ان ينتج مجال انضغاطي على شكل قنينة وخاصة في حالة كون عرض التحميل هو اقل من عرض العضو الانشائي الساند. في مختبر قسم هندسة البناء والانشاءات- الجامعة التكنولوجية سلسلة من الفحوصات المختبرية قد تمت لنماذج خرسانية متعرضة الى قوى انضغاط لتكوين مجال انضغاطي. المتغيرات المأخوذة هي محتوى الالياف، مقاومة الانضغاط للخرسانة، تسليح الشد العرضي، ارتفاع النموذج، نسبة عرض بليتة التحميل الى عرض النموذج. تم دراسة تأثير هذه المتغيرات على قابلية الاسناد لمحتوى الانضغاط الذي يكون على شكل قنينة. تم فحص تسعة نماذج ، ثمانية منها مسلحة بالالياف وواحد فقط غير مسلح بالالياف.

بالاعتماد على نتائج الفحوصات المختبرية ، كل النماذج المفحوصة فشلت بالانشطار تحت بليتة التحميل مباشرة . زيادة مقاومة الانضغاط للخرسانة يزيد اجهادات الاسناد للانضغاط. العلاقة بين القوة والتشوه العرضي يتصرف بالبداية خطي ولكنه يكون غير خطي قبل الفشل. اضافة الياف الحديد للخرسانة العادية او اضافة تسليح عرضي يؤخر الوصول الى اعلى اجهاد الاضغاط بعد ظهور التشقق الاولي.

الكلمات الرئيسية: خرسانة مسلحة بالالياف، اجهادات الانضغاط ، مجال الانضغاط على شكل قنينة .

1. INTRODUCTION

A normal strength concrete considers as a brittle material with high compressive strength in comparison with the low tensile strength. To increase the tensile strength of concrete, small pieces of fibres could be added to concrete members. Fibers are classified according to its nature of the material (e.g. steel, glass, polymer and carbon). Steel fibers are usually short with the aspect ratio between 30 to 200. It will combine with concrete and they are randomly distributed **Craig, 1984**.

One of the main reasons to use the steel fibres in structural concrete is crack arrestors through the bridge process. Also, using steel fibres will increase the ductility and toughness and the possibility of shrinkage of concrete will be reduced.

The degree of improvement of the mechanical properties of concrete by addition of steel fibres is dependent on the shapes, aspect ratio and steel fibres content.

Meanwhile, the main disadvantage of steel fibre reinforced concrete (SFRC) is the difficulties of mixing the fibres into concrete which affected by the orientations and segregation of fibres.

Internal strut in a compression member may take the shaped of prismatic or bottle-shaped, as shown in **Fig. 1**. The Bottle-shaped struts are thinner at the ends and wider at the mid-height. The compression stresses spread parallel to the strut, meanwhile, tensile stresses developed perpendicular to the direction of the strut, which results in longitudinal cracks.

Most of the researchers preferred to idealize the bottle-shaped compression field with a prismatic section with a linearly tapered section at the ends with a slope of 1:2 as shown in Figure 1b. The strength of the strut depends on the effective compressive strength of concrete. To avoid the longitudinal cracks due to transverse tensile stresses, reinforcement is added parallel to the direction of the strut, **James** and **James, 2012**.

The main objectives of this study are:

- Study the mode of failure of fibre reinforced concrete (FRC) members subjected to compressive stresses.
- Study the effect of compressive strength of concrete, fibre content, the ratio of the width of loading plate to the width of concrete member, the height of concrete member, and presence of transverse reinforcement on bearing capacity of compression field of fibre reinforced concrete member.

2. MATERIAL AND MIX PROPORTIONS

The following materials were used in the present investigation: Ordinary Portland cement –type I with specific gravity 3.15; Coarse aggregate, 5-19 mm size aggregate with specific gravity 2.62; fine aggregate, manufactured sand with specific gravity 2.57 and fineness modulus 3.05.

Three different compressive strength of concrete (fc=13.4, fc=30.4 and fc=50.7) were proposed and at least three samples of 10x20 cm cylinder were used to measure the compressive strength of concrete at 28 days according to ASTMC39. The compositions of the mix design adopted for the present investigation are presented in **Table 1**.

3. EXPERIMENTAL PROGRAM

The experimental program was conducted in the laboratories of Building and Construction Department- University of Technology-Iraq.

A total of ten cubes were tested: nine was made from normal strength concrete with steel fibre and one was made from normal strength concrete without steel fibre.

The influence of steel fibres on bearing capacity of compression field was studied on three specimens (C1-0F, C2-0.5F and C3-1.2F). The compressive strength of concrete was studied by comparisons of three specimens (C2-0.5F, C6-fc13 and C7-fc50). The ratio of the width of loading plate to the width of the specimen was investigated by four specimens (C2-0.5F, C4-10b/a, C5-2b/a and C10-1.5b/a). The effect of the height of concrete specimen was studied by comparison of two specimens (C2-0.5F and C8-h60). Finally, the effect of the presence of transverse reinforcement on bearing capacity of compression field was investigated by comparisons of two specimens (C2-0.5F and C9-TR). The characteristics of tested specimens were presented in **Table 2**. In this table, $f_{c'}$ represents the compressive strength of cylinder at 28 days. b/a represents the ratio between the width of the specimen to the width of loading plate.

4. GEOMETRY OF TESTED SPECIMEN

All the tested specimens had a cubic shape with 30x30x30 cm long side; only the specimen of C8-h60 had a height of 60 cm to study the effect of the height of specimen on bearing capacity of compression field.

5. STEEL FIBER

Fig. 2 shows the steel fibre type that was used in this study. This fibre has a length of 15 mm, the diameter of 0.20 mm and the aspect ratio is 75.

6. TEST SETUP

The tests were carried out using the hydraulic jacks of 2500 kN in the laboratory of the building and construction department at the University of Technology-Iraq as shown in **Fig. 3**. The specimens were subjected to compressive stresses using 5 cm plate thickness.

7. MEASUREMENTS

The applied load was measured using an accurately calibrated load cell. The vertical displacement at the top and bottom (point 4) of the specimens was measured using dial gauge. The horizontal displacements in three locations (points 1,2 and 3) were also measured using dial gages as shown in **Fig. 4**.

8. CURING PROCESS

The specimens were placed in the water tank with an average temperature of 22 °C for 28 days. After that, the specimens were laid in the laboratory temperature until the date of testing.

9. TESTING PROCEDURE

Before testing, the dial gauges were adjusted and checked; as shown in **Fig. 5**. The vertical load was applied to the specimens by load increments of 5 kN.

In all tests, loading was continued till the peak load (ascending part) to clearly see the whole crushing of concrete specimens. In this research, descending part is not an important consideration in bearing capacity of compression field. Cylinder compressive tests were carried out approximately on the same day as the corresponding specimen test. As the crushing of concrete was completed, the load was removed to allow more photographs of the final cracks and failure patterns to be taken. The time spent in testing one specimen was about 15 to 20 minutes.

10. RESULTS AND DISCUSSIONS

This section presents test results of first crack load, the effect of fibre content, the effect of b/a ratio, the effect of compressive strength of concrete, the effect of specimen height and the effect of the presence of transverse reinforcement on compressive strength of bottle-shaped compression field. Also, the load-transverse deformation behaviour, load-vertical deformation behaviour, and modes of failure were presented.

10.1 The Effect of Fiber Content on Bearing Capacity of Compression Field

As mentioned before, the test specimens have three fibre contents, first with 0% fibre content (C1-0F), second with 0.5% fibre content (C2-0.5F) and third with 1.2% fibre content (C3-1.2F).

By keeping b/a constant (b/a=5) and changing only the fibre content, the maximum compressive stresses $\sigma_{c,max}$ is calculated which is represented by the applied load divided by and the area of loading plate.

As expected, the ratio of $\sigma_{c,max}/f_c$ increased by 1.6% when the steel fibre content increased from 0% to 0.5%, while this ratio increased by 8% when the steel fibre content increased from 0.5% to 1.2% as listed in **Table 3**. This may be due to the fact that the steel fibre arrested the opening of the cracks through the bridging process which causes an increase in the maximum compressive stresses.

10.2 The Effect of b/a on Bearing Capacity of Compression Field

The test results of the effect of the width of the test specimen (b) to the width of loading plate (a) are represented by (b/a) on bearing capacity of compression field are summarized in **Table 4**. As expected, for b/a= 1, the value of $\sigma_{c,max}/f_c$ equal to 1. From **Table 4**, with an incremental increase of b/a, the value of $\sigma_{c,max}/f_c$ decrease till reaching the minimum value, then increased till reaching the values more than fc. The whole behaviour of the effect of b/a on the ratio of σ_c/f_c is shown in **Fig. 6**. The reasons of that are, for high b/a, the effective width of bottle-shaped at the mid-height of the specimen is small producing compressive stresses beyond the transverse tensile stresses increased the bearing capacity of compression field.

10.3 The Effect of Compressive Strength of Concrete on Bearing Capacity of Compression Field

The three tested specimens as mentioned before have three uniaxial compressive strength of 13.4, 30.4 and 50.7 MPa for C6-fc13, C2-0.5F and C7-fc50 specimens respectively. AS expected, by increasing the uniaxial compressive strength of concrete from 13.4 to 50.7 MPa, the ratio of $\sigma_{c,max}/f_c$ decreases from 0.78 to 0.49 respectively (see **Table 5**).

10.4 The Effect of Specimen Height on Bearing Capacity of Compression Field

To study the effect of the height of specimen on bearing capacity of compression field, two specimens were constructed, first; specimen of 30 cm height (C2-0.5F) and a second specimen of 60 cm height (C8-h60). The test results are summarized in **Table 6**. When the height of specimen is doubled the bearing capacity of compression field is increased by 32.3% and the ratio of $\sigma_{c,max}/f_c$ is also increased. The reason of that is, increase the height of concrete specimen means increased the path of concrete resistance up to failure.

10.5 Transverse Reinforcement Effect on Bearing Capacity of Compression Field

To study the effect of transverse reinforcement on bearing capacity of compression field, the C9-TR specimen transversely reinforced with 7-ϕ6mm diameter equally spaced in the middle of the specimen (exactly in the maximum transverse tensile stresses of bottle-shaped). **Table 7** summarized the test results, in which, the transverse reinforcement increases the ratio of $\sigma_{c,max}/f_c$ by more than two times. This is because of the resistance of transverse reinforcement to maximum transverse bottle-shaped tensile stresses in the middle of the specimen.

11. LOAD-TRASVERSE DEFORMATION BEHAVIOR

As stated before, the horizontal dial gauges were used to measure the horizontal displacement at a quarter (point 1 and 3) and at middle height (point 2) of the specimen as stated in **Fig. 4**. The relation between $\sigma_{c,max}/f_c$ and the transverse displacements were illustrated in **Fig. 7** to **Fig. 11**.
Disregarding some nonlinearities at the beginning of testing resulting from the test setup, the load-transverse deformation behaviour of tested specimens was initially linear till about 93% of the maximum stresses and then nonlinear behaviour pronounced till the maximum compressive stresses. The softening zone after reaching the maximum compressive stresses will be disregarded because it is beyond the scope of this work.
By comparisons with the reference specimen (C2-0.5F), as shown in **Fig. 7** to **Fig. 11**, the differences of measurement in transverse displacement between dial gauges placed at point 1 or 3 and dial gauge placed at point 2 confirm the distribution of compressive stresses in bottle-shaped.
Also, the test results of transverse displacement at mid-height shows the biggest width of bottle-shaped occurs at the C4-10b/a (specimen with less width of loading plate). And, the less width of bottle-shaped of compression field occurs at C3-1.2F specimen (with 1.2% fibre content). The specimen C7-fc50 (specimen with compressive strength 50.7 MPa) shows the more nonlinear behaviour before failure.

12. LOAD-VERTICAL DEFORMATION BEHAVIOR

As previously pointed, the dial gages also used to measure the vertical displacement at the edge of specimens. The relations between the $\sigma_{c,max}/f_c$ and the vertical displacement is illustrated in **Fig. 12**.

13. MODES OF FAILURE

The bearing failure of compression field for all tested specimens is splitting type of failure. Splitting started with a crack under the edges of load application area due to load concentration there. Sometimes two splitting cracks developed. **Fig. 13** shows the modes of failure for tested specimens

14. CONCLUSIONS

- Addition of steel fibre to normal strength concrete or presence of transverse reinforcement increases the maximum bearing capacity of compressive strength of the specimen.
- Increased the uniaxial compressive strength of concrete increases the maximum bearing capacity of compressive stresses.
- The load-transverse deformation initially behaves linearly and shows some nonlinearity before failure.
- With incremental increasing the ratio of b/a, the value of $\sigma_{c,max}/f_c$ decrease till reaching the minimum value, then increased till reaching the values more than f_c.
- The dial gauges measurements in transverse direction confirm the bottle-shaped compression stress distributions.
- The bottle-shaped compression field failed with the splitting type of failure due to load concentrator.

REFERENCES

- AASHTO, 2007, *LRFD Bridge Specifications*, 4th Edition, American Association of State Highway and Transportation Officials.
- Al-Quraishi H., 2014, *Punching Shear Behavior of UHPC Flat Slabs*, PhD Thesis, Kassel University-Germany.
- Craig, J., 1984, *Structural Applications of Reinforced Fibrous Concrete*, ACI Concrete

International, P.P 40-46.
- Gary K., 2008, *A detailing tool for Strut and Tie Model*, Concrete International, American Concrete Institute.
- James W. and James M., 2012, *Reinforced Concrete Mechanics and Design*, Text Book, Sixth Edition.
- Jörg S. and Dieter W., 1982, *Detailing of Concrete Structures*; Comite Euro-International du Beton, Paris.
- Jörg, S. and Kurt S., 1991, *Design and Detailing of Structural Concrete Using Strut and Tie Models*, the Structural Engineering, Vol.69, No.6, P.P 46-62.
- Perry A. and Zongyu A., 1993, *Bearing Strength of Compressive Struts Confined by plain Concrete*, ACI Structural Journal, Vol.90, No.5, P.P 112-116.
- Torsten L. and Ekkehard F., 2012, *Compressive Strength of UHPC in Bottle-Shaped Compression Field*, International Symbision in Kassel University-Germany, P.P 96-104.

Table 1. Compositions of concrete mix design.

Mtaerials (kg/m^3)	$f_{c'}$=13.4	$f_{c'}$=30.4	$f_{c'}$=50.7
Cement (kg/m3)	338.2	472.8	788.1
Fine aggregate	1003.4	868	553.1
Coarse aggregate	967.2	967.2	967.2
Water	236	236	236
W/C	0.7	0.5	0.3

Table 2. Details of tested specimens.

Specimens Designation	Concrete Type	$f_{c'}$ (MPa)	fiber content (%)	b/a	Height of specimen (cm)	Width of loading plate (cm)	Transverse reinforcement
C1-0F	NSC	29.6	0	5	30	6	-
C2-0.5F	NSC	30.4	0.5	5	30	6	-
C3-1.2F	NSC	32.1	1.2	5	30	6	-
C4-10b/a	NSC	30.4	0.5	10	30	3	-
C5-2b/a	NSC	30.4	0.5	2	30	15	-
C6-fc13	NSC	13.4	0.5	5	30	6	-
C7-fc50	NSC	50.7	0.5	5	30	6	-
C8-h60	NSC	30.4	0.5	5	60	6	-
C9-TR	NSC	30.4	0.5	5	30	6	7-ϕ6mm
C10-1.5b/a	NSC	30.4	0.5	1.5	30	20	-

Table 3. Maximum compressive stresses at failure.

Specimens	f_c' (MPa)	$\sigma_{c,max}$ (MPa)	$\sigma_{c,max}/f_c'$
C1-0F	29.6	18.3	0.61
C2-0.5F	30.4	19	0.62
C3-1.2F	32.1	21.6	0.67

Table 4. Effect of b/a on bearing capacity of compression field.

Specimens	$f_c^{'}$	b/a	a (cm)	$\sigma_{c,max}/f_c^{'}$
C4-10b/a	30.4	10	3	1.56
C2-0.5F	30.4	5	6	0.62
C5-2b/a	30.4	2	15	0.75
C10-1.5b/a	30.4	1.5	20	0.82

Table 5. Effect of compressive strength of concrete on maximum compressive stresses.

Specimens	$f_c^{'}$ (MPa)	$\sigma_{c,max}$ (MPa)	$\sigma_{c,max}/f_c^{'}$
C6-fc13	13.4	10.5	0.78
C2-0.5F	30.4	18.8	0.61
C7-fc50	50.7	25	0.49

Table 6. Effect of height of specimen on maximum compressive stresses**.**

specimens	$f_c^{'}$ (MPa)	$\sigma_{c,max}$ (MPa)	$\sigma_{c,max}/f_c^{'}$
C2-0.5F	30.4	18.8	0.61
C8-h60	30.4	27.8	0.91

Table 7. Effect of transverse reinforcement of specimen on maximum compressive stresses.

Specimens	$f_c^{'}$ (MPa)	$\sigma_{c,max}$ (MPa)	$\sigma_{c,max}/f_c^{'}$
C2-0.5F	30.4	18.8	0.61
C9-TR	30.4	44.4	1.46

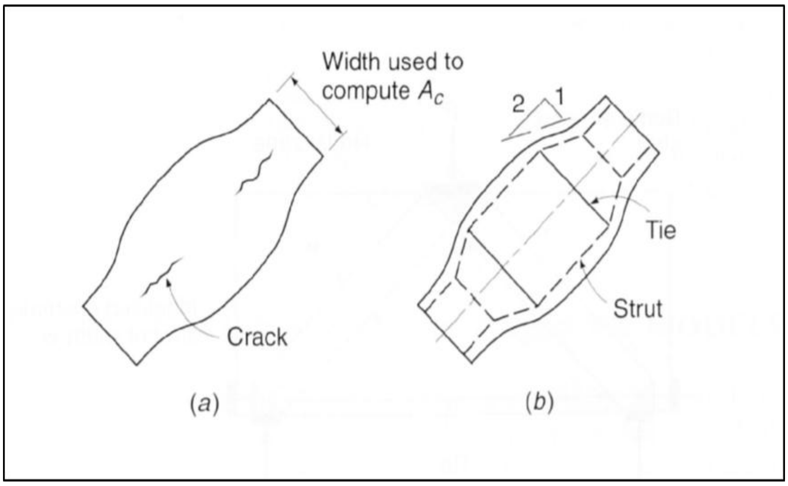

Figure 1. Bottle-shaped strut.

Figure 2. Steel fibre used in constructed the specimens.

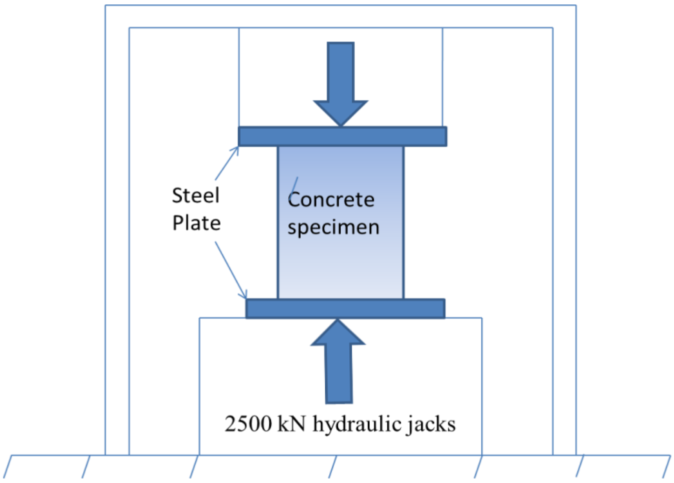

Figure 3. Test Setup.

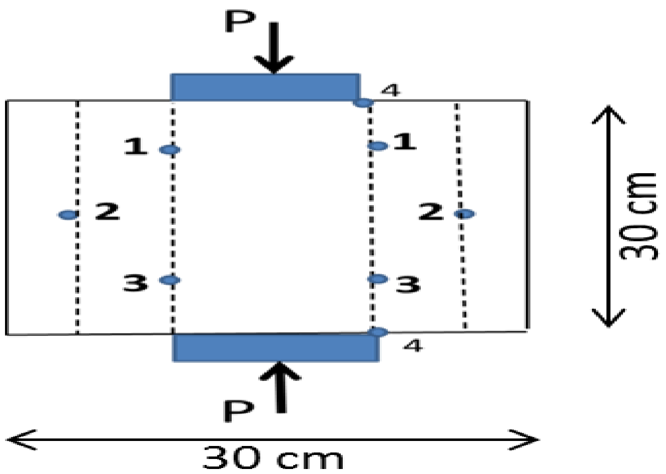

Figure 4. Points of measurement.

Figure 5. Specimen under test.

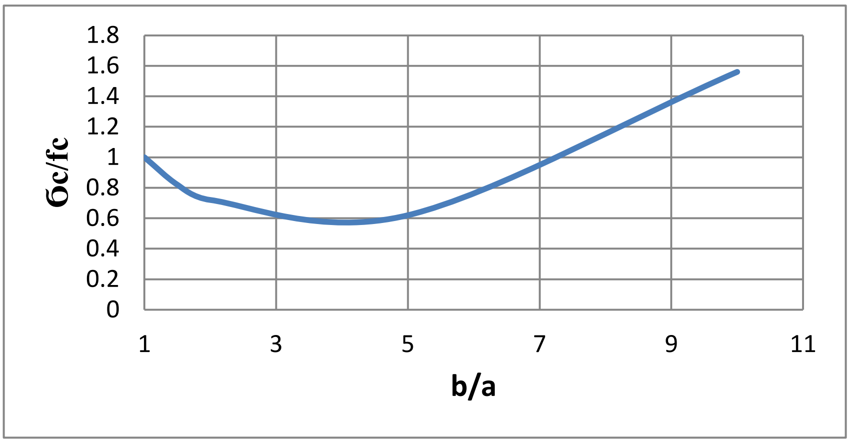

Figure 6. The relation between the $Ϭ_c/f_c$ with the b/a.

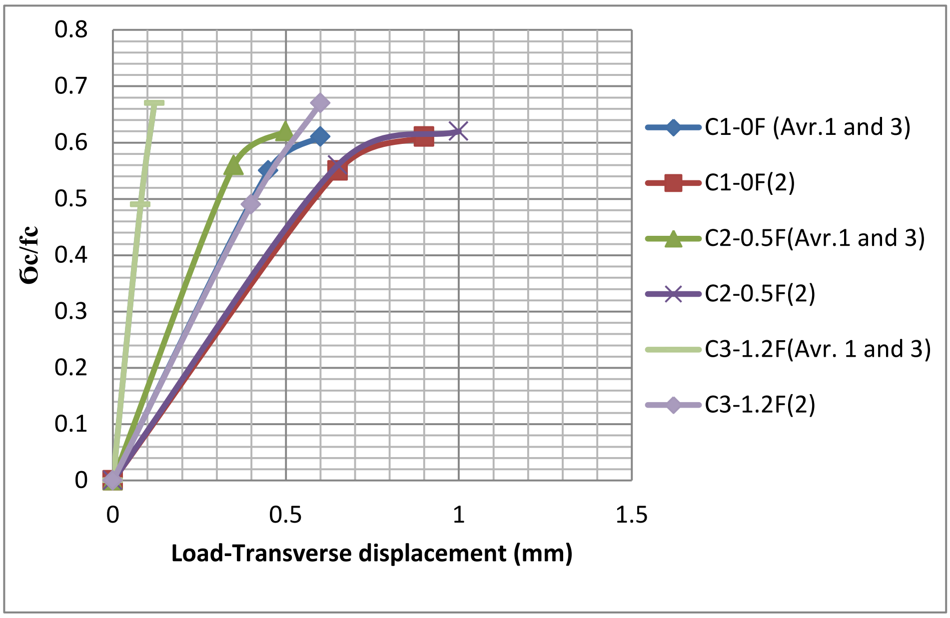

Figure 7. Load-Transverse displacement of C1-0F, C2-0.5F and C3-1.2F specimens.

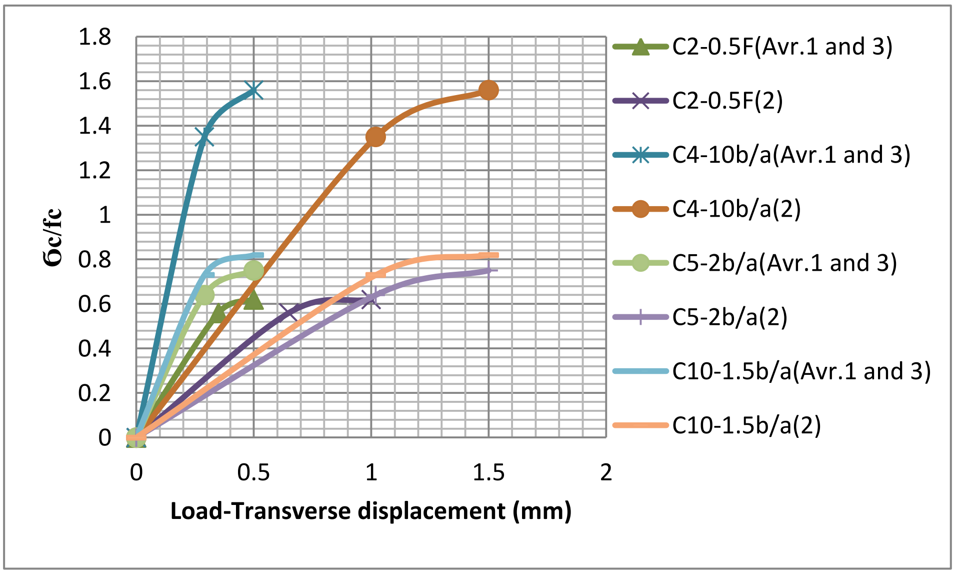

Figure 8. Load-Transverse displacement of C2-0.5F, C4-10b/a, C5-2b/a and C10-1.5b/a Specimens.

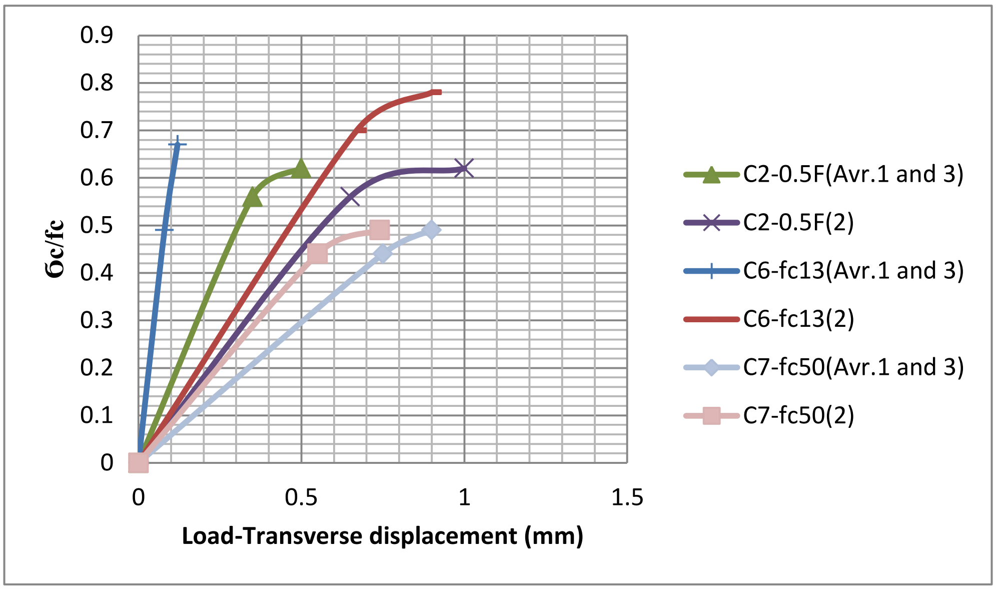

Figure 9. Load-Transverse displacement of C2-0.5F, C6-fc13 and C7-fc50 specimens.

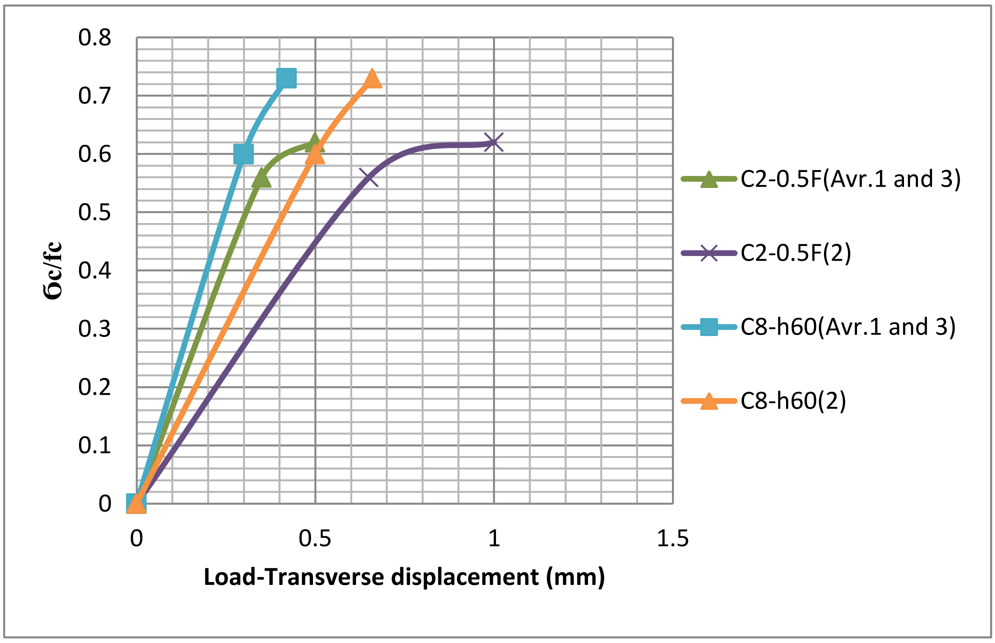

Figure 10. Load-Transverse displacement of C2-0.5F and C8-h60 specimens.

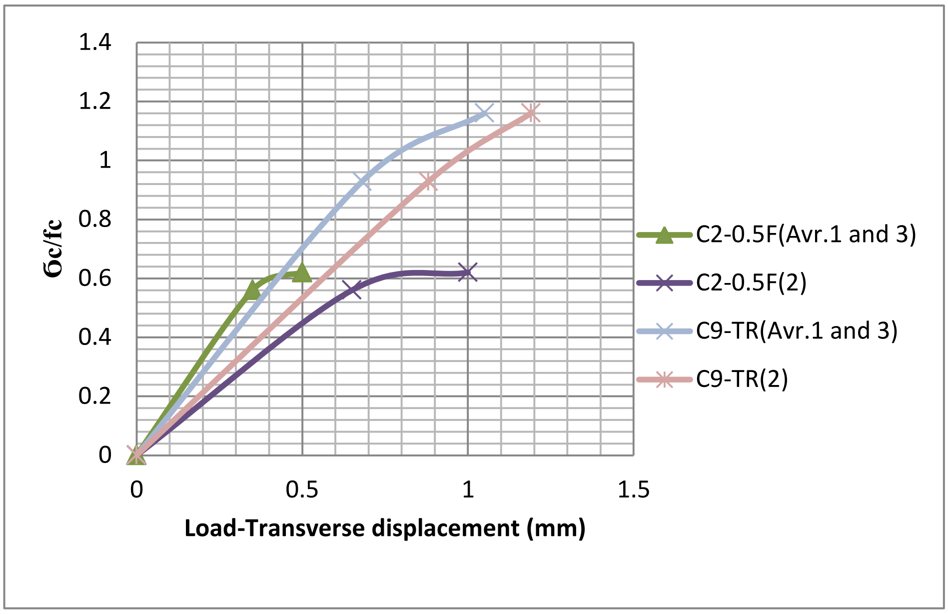

Figure 11. Load-Transverse displacement of C2-0.5F and C9-TR specimens.

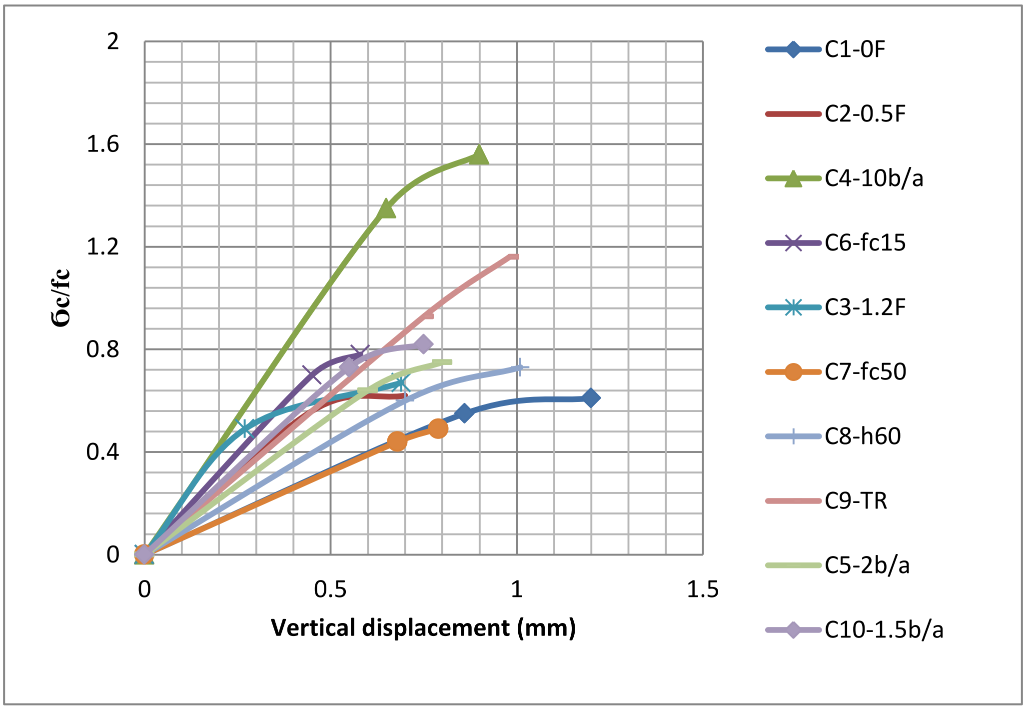

Figure 12. Vertical displacement of tested specimens.

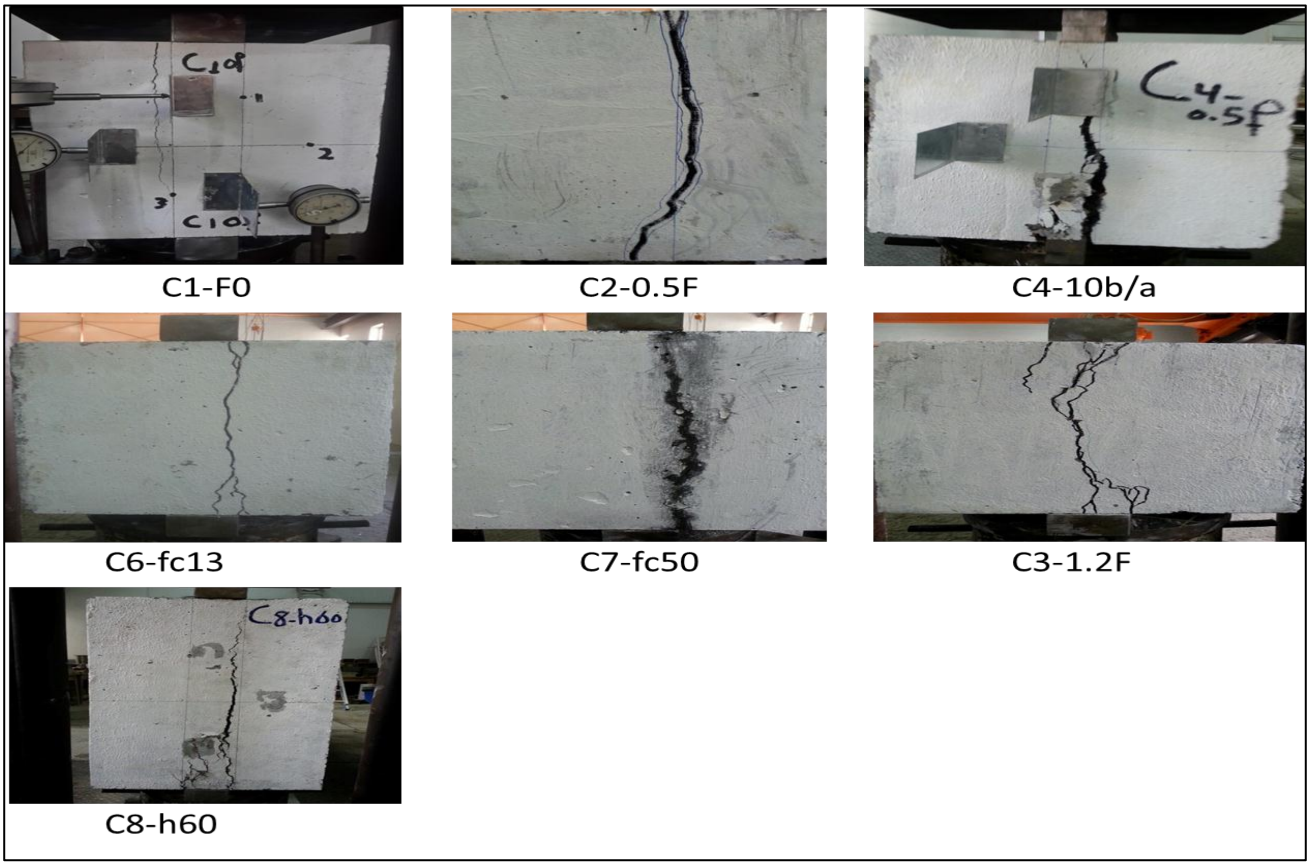

Figure 13. Mode of failure of tested specimens.